

Energy Effect of Laser-induced Vertical Metallic Link

Wei Zhang, Joo-Han Lee, and Joseph B. Bernstein, *Member, IEEE*

Abstract—In this paper, the energy effect of the laser vertical metallic link is investigated from a microscopic point of view through experimental observations and simulations. Sample structures that were irradiated under different laser energies were cross-sectioned and observed using a FIB/SEM dual beam system. Failure criterion at the high energy was defined by excessive material loss in the lower metal (metal 1) and passivation cracking. Micro-images also suggest that for an optimal link structure, the upper metal (metal 2) opening should be larger than the lower metal line-width considering the dielectric-step-induced lens effect. Taking into account both measured electrical resistance and observed voids in the lower metal, the normalized energy process window is defined to be the absolute energy range divided by the average energy. For the structures with 1 μm , 2 μm , 3 μm and 4 μm lower metal line-widths, the relative process windows are 0.83, 0.87, 0.9 and 0.96, respectively. Simulations also revealed consistent results with the experimental observations, which is a monotonically decreasing trend of relative energy process windows for more scaled links. A simple equation to evaluate the spot size of laser beam for various link structures is presented. These results demonstrate the application of commercially viable vertical linking technology to VLSI applications.

Keywords—Energy process window, interconnect density, laser antifuse, laser processing, make link, scalability, yield enhancement.

I. INTRODUCTION

SINCE the laser-induced vertical metallic link has been proposed as a programmable element, efforts have been made to investigate its acceptability for practical applications [1], [2]. As a complementary scheme to the metal fuse, the laser vertical metallic link has been reported to be superior to conventional metal fuse for its hermetic metal after laser processing, higher yield [3] and denser integration potential [4], [5], which indicate strong potential for far-reaching practical restructuring applications in the semiconductor industry.

Figures 1 and 2 show the schematics of top and cross-sectional views of the link structure and a cross-sectional focused ion beam (FIB) image of a processed link site. Previously, accelerated electromigration tests were performed to investigate the reliability of link. In that work, laser-induced voids in the lower metal (metal 1) were revealed as an inherent defect and an ultimate lifetime limiting factor of the link due to the void migration and nucleation in the metal 1 [3].

Further understanding of the kinetics of electromigration led to a design of a special link structure and suggested that electromigration in the link sheets would not be critical

compared with that in metal 1. This phenomenon was attributed to the metal atom back-diffusion or “Blech effect” [6]. Obviously, one can reduce the void size by cutting down the incident energy of the laser beam. However, insufficient energy will result in undesirable thin link sheets and high electrical resistance. Counterbalance of the two effects is the only way to optimize the laser process conditions. The quality of linking process is affected by a variety of factors and they include the shape and length of laser pulse, the spot size and laser alignment accuracy. Among the various laser parameters for laser processing using commercial *Q*-switched laser positioning systems, the laser energy is the most important factor, which can control directly the metal melting as well as dielectrics cracking through the thermal expansion of metal.

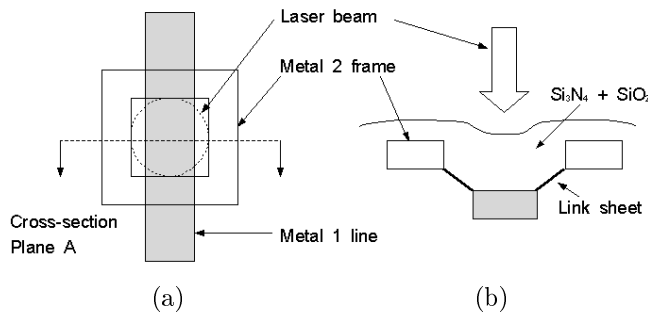


Fig. 1. Schematic of a vertical link structure after a laser pulse, (a) layout and (b) cross-section from Plane A.

On the other hand, because the density of memory cells has been of primary importance in reducing their cost, the reduction in cell size has been achieved by the use of smaller interconnect line width as well as by the cell structure complexity [7]. With this continuous shrinking of device dimensions of Si MOS technologies, the scaling down of link structures has become a primary issue in practical applications. The scalability of a vertical link structure was estimated and shown to be compatible with the current semiconductor technologies in [4].

In this work, the effects of laser energy on the void distribution in metal 1 will be detailed through FIB image observations. Then, laser process windows in term of the energy range for acceptable link formation will be shown for four different sizes of link structures considering both measured resistance and FIB failure analysis. Also, an analysis of the linking process for shrunken link structures by finite element modeling, showing the consistent trend with experimental results, will be presented. And through the comparison of experimental and simulation results, the scalability of a vertical make link will be discussed. Fi-

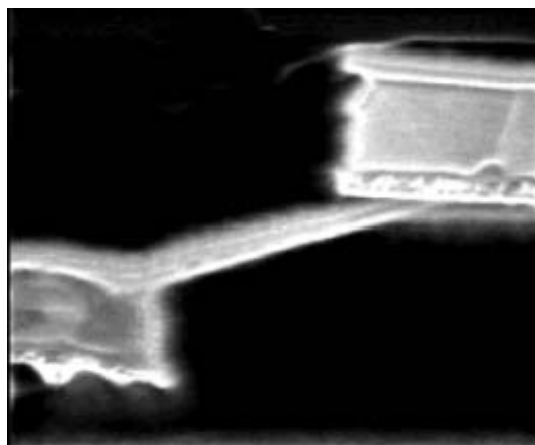


Fig. 2. FIB cross-sectional image of a vertical link (the picture shows only half structure).

nally, a study of linking processes on two structures, with and without a lateral gap from metal 1 to metal 2, will be addressed.

II. EXPERIMENTAL

The samples were fabricated using a standard 2-level metal CMOS process. The two levels of metallization are aluminum based with 1 % silicon and 0.5 % copper. The thicknesses for metal 1 and metal 2 are 0.6 and 0.8 μm , respectively. The aluminum alloy was deposited on a field oxide grown on the silicon substrate. There was an inter-level dielectric (ILD) consisting of PECVD SiO_2 (TEOS) between the two levels of metallization. The metallization was formed by sputtering and contained a thin undercoating of TiN and an overcoating of Ti. TiN undercoating layer provides good contact with metal 1 and it also acts as a diffusion barrier that can increase the electromigration reliability of the link. The overcoating Ti layer is an anti-reflective coating to increase the efficiency of future lithography steps and it also improves the laser energy absorption in the metal during laser processing.

Metal 2 was coated with SiO_2 followed by a Si_3N_4 passivation. The dielectric is expected to exhibit a room temperature compressive stress of about 200 MPa or less to the aluminum. In this study, totally five sample structures (cells) were investigated as listed in Table I. Although the line width of metal 1 and the size of the metal 2 opening were different for each sample, the width of metal 2 frame was the same (2 μm).

It is noted that the top-layer metallization and the next one have been defined as metal 2 and metal 1 respectively for the sake of simplicity throughout this paper, though they are metal N and metal N-1 in the current multi-level metallization, where N is the total number of metal layers.

The laser system used to perform the linking of Samples 1 to 4 was an *XRL 525* laser process system. The system employs a *Spectra Physics* diode-pumped, *Q*-switched, Nd:YLF laser operated in the saturated single-pulse mode. IR laser pulses with a series of energies were directed to

TABLE I
CELL STRUCTURAL PARAMETERS OF THE VERTICAL LINK TEST CHIP
(UNIT : μm)

Sample	metal 2 opening size	metal 1 line width
Sample 0	2.2×2.2	1.2
Sample 1	4×4	2
Sample 2	4×4	3
Sample 3	4×4	4
Sample 4	6×6	4

each link structure of Samples 1-4. On the other hand, links of Sample 0 were processed utilizing a *ESI 9200HT PLUS* laser process system, which is a more advanced system with better alignment accuracy and repetition rate. Each link of all samples throughout this experiment was exposed to a single laser pulse focused on metal 1 with a wavelength of 1.047 μm and a pulse length of 15 ns. The laser spot size defined to be the $1/e^2$ diameter which was set equal to about twice the line width of metal 1, so approximately 50% of laser energy could be delivered on to top of metal 1 through the metal 2 opening. Processed samples were examined both electrically and microscopically to see the connections of the link structures.

III. RESULTS AND DISCUSSION

A. Energy effect

The sample link structures with a $4 \times 4 \mu\text{m}$ opening on a metal 2 frame and a 2 μm wide metal 1 line (Sample 1) were irradiated with an energy range of 0.11-0.8 μJ and a 3.4 μm spot size in $1/e^2$ diameter. The FIB cross-sectional images of Sample 1 links processed with various energies are shown in Fig. 3, 4 and 5.

At the lowest available energy of 0.11 μJ , the dielectric has already been fractured by thermal expansion of metal 1 and a thin link sheet formed between the metal 1 line and the metal 2 frame, while leaving several small voids in the lower metal. The dielectric cracking and the molten metal filling was initiated from the upper corners of the metal 1 line and ended at the lower corners of the metal 2 frame. In theory, the crack initiation and propagation involve many complicated factors. For brittle materials, the maximum principal tensile stress is generally responsible for the crack initiation [8]. The initiation point of cracking and the propagation path are largely controlled by the stress concentration. Finite element analysis indicates the trajectory of a dielectric crack under a laser pulse of fixed length is independent of laser energy, which is consistent with our experimental observations.

As the energy increases, the link sheet becomes thicker at a cost of leaving more voids in the metal 1 line. One can trace the metal melting front by the void distribution in metal 1. Figures 3 to 5 display the changes of the void distribution in metal 1 with an increase of the laser energy. At an energy of 0.11 μJ , the voids are located only near the

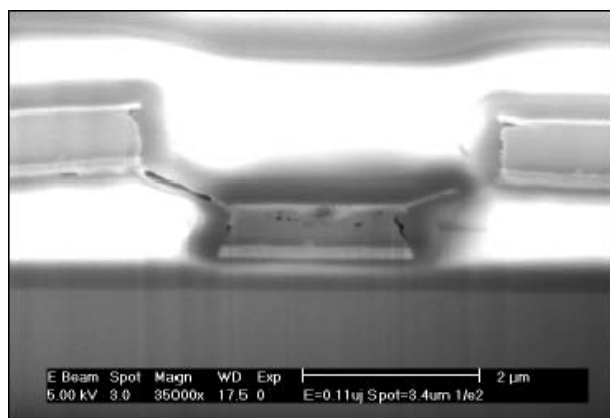
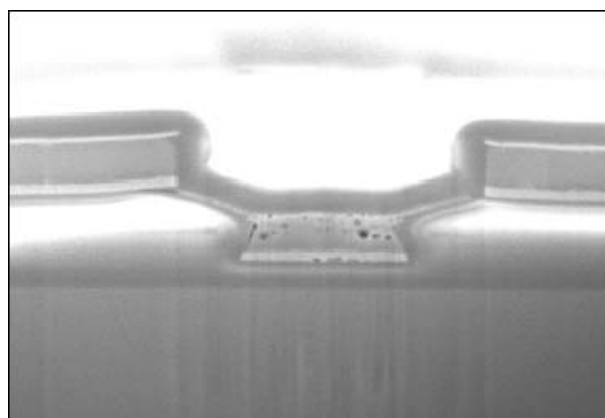
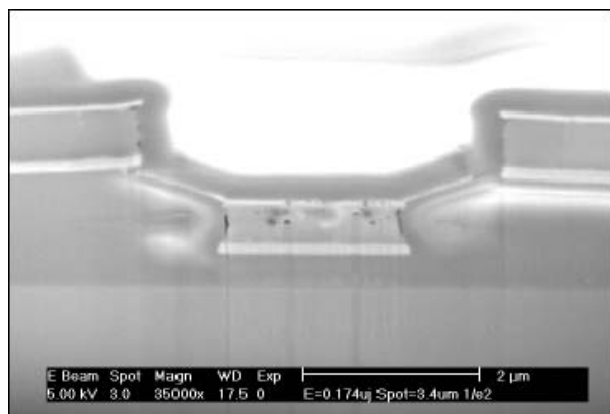
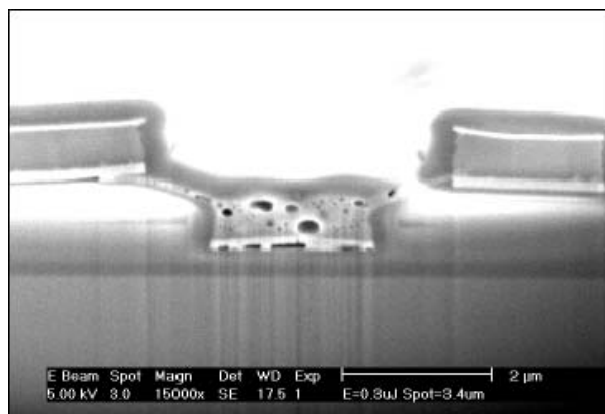
(a) Energy = 0.11 μJ (a) Energy = 0.24 μJ (b) Energy = 0.17 μJ (b) Energy = 0.30 μJ

Fig. 3. Vertical link formation and voiding effect at different laser energies 1, Sample 1.

Fig. 4. Vertical link formation and voiding effect at different laser energies 2, Sample 1.

top surface of the metal 1 line, while the voids can be found in the middle of metal 1 at an energy of 0.17 μJ . When the energy was increased to 0.24 μJ , some small voids are observed even in the TiN undercoating layer. Considering the high melting point of TiN, the voids presented in TiN layer may be caused by TiN peeling-off, rather than melting. When the laser energy is 0.30 μJ , voids are distributed everywhere in metal 1 as shown in Fig. 4 (b). Therefore, the melting front reached the bottom in the case of laser pulse with an energy of 0.30 μJ , while only the top part of metal 1 was molten at the end of the 15 ns laser pulse with an energy of 0.11 μJ .

Continuously increasing the laser energy can not only deplete the metal 1 line, but also crack the top passivation and void the upper metal frame. A cross-sectional image of the link site processed with an energy of 0.49 μJ is shown in Fig. 5 (b). It is clear that the link failed because of severe voids in the metals and cracked passivation. It has been observed that passivation starts to rupture from an energy of 0.51 μJ or so. Although electrical measurement may still show reasonably low resistance at such a high energy, the link process is considered as a failure with regard to electromigration reliability. Therefore, results suggest that thickening the link sheet by simply increasing laser energy

will not proportionally improve the overall reliability of the link. Consequently, the high end of the energy process window should be defined by the onset of the passivation cracking or excessive voiding in metal 1, rather than the passivation rupture.

Average electrical resistance values for sample numbers 0, 1, 2 and 4 were obtained and reported in [1] and [4]. The energy ranges for the four structures to form acceptable links were obtained from the electrical measurements and microscopic analysis and are summarized in Fig. 6. It is clear that larger size structures (wider metal 1 line) have broader energy windows. [4]. However, the process window in term of absolute energy lacks universal significance and, thus a normalized window is preferred. Now the processing window is redefined as the ratio of the difference between the high and the low energies ($E_h - E_l$) to the average energy (E_a).

$$\text{Relative Process Window} = \frac{E_h - E_l}{E_a}$$

The relative window is a normalized, non-dimensional term that eliminates the dependence of the absolute energy window on the characteristics of different laser systems.

As can be seen in Fig. 6, the absolute energy range

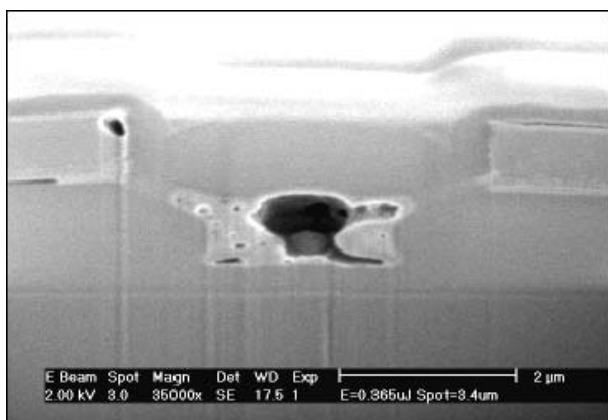
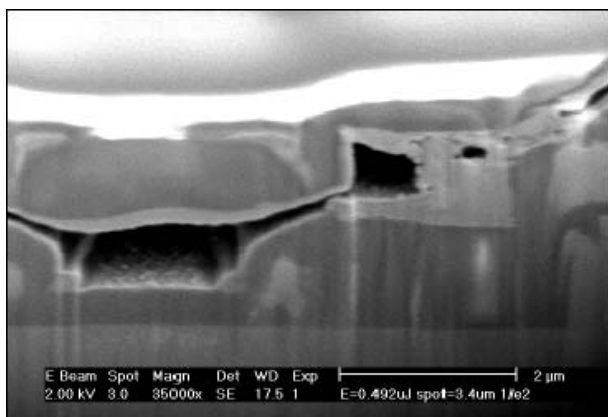
(a) Energy = 0.37 μJ (b) Energy = 0.49 μJ

Fig. 5. Vertical link formation and voiding effect at different laser energies 3, Sample 1.

(presented by error bars) decreases with the reduced metal 1 width for Samples 0, 1, 2 and 4 (shown as metal 1 widths of 1.2, 2, 3 and 4 μm in X axis), while an exception is found for Sample 0. The upward shift in energy bounds for Sample 0 is attributed to the calibration difference in relative energy between *XRL 525* and *ESI 9200HT PLUS* laser process systems. The relative laser energy windows, plotted in Fig. 6, demonstrate monotonically increasing process window with increased link size. For the structures with 1.2, 2, 3 and 4 μm wide metal 1 lines, the relative process windows were 0.83, 0.87, 0.9 and 0.96. This result indicates that the scaling-down of the link size will raise the requirements on both positioning accuracy and energy stability of the laser system. Nonetheless, the normalized energy window extrapolates to no less than 0.75 for a zero width (hypothetical) metal 1 line and thus, we can conclude that an acceptable energy window will always be found for the metal link process for aluminum lines insulated by silicon oxide dielectric.

IV. FINITE ELEMENT SIMULATIONS

To simulate the make-linking process, a finite element model, MSC *Mentat* was used. The energy process window from experimental observations were compared with

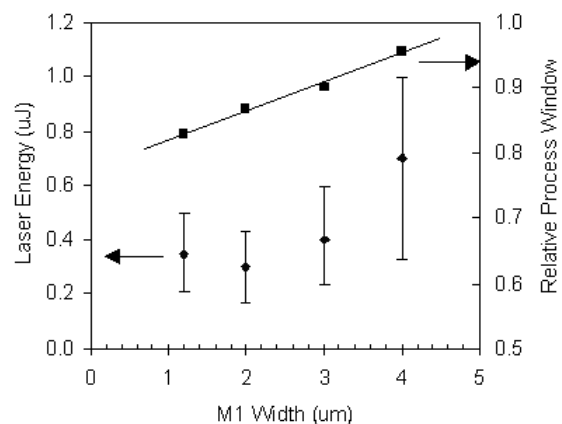
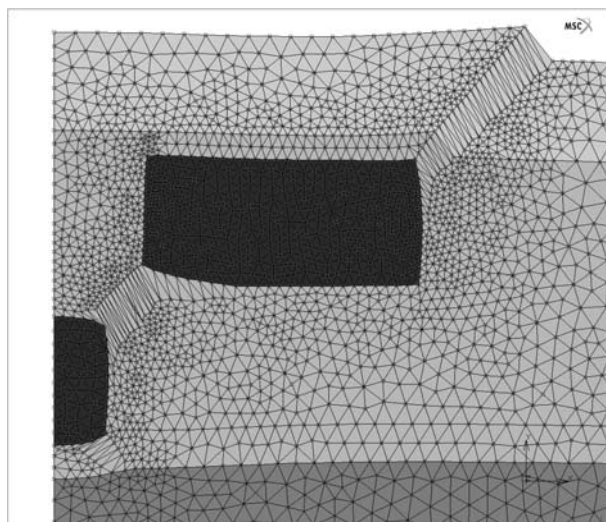


Fig. 6. Available laser energy range and relative process windows for various link structures, Samples 0, 1, 2 and 4.

2-dimensional simulations. The energy process window for various make-link structures were conducted assuming no laser positioning error.

Fig. 7 displays the results of finite element modeling of the cross section of failed scaled make link caused by a laser energy above the high end of energy process window. It shows the cracked passivation caused by the thermal expansion of metal 2 frame which is heated by absorption of laser energy. The width of metal 1 was 0.5 μm and the 2 μm wide frame of metal 2 had a 1.5 \times 1.5 μm square opening. Due to the high energy absorbed in metal 1 and metal 2, the cracking of dielectric can be observed on upper and lower corners of metal 1 line as well as the upper corner of metal 2.

Fig. 7. Results of finite element analysis showing passivation cracking caused by a laser energy above the high end of process window, scaled link structure with 1.2 μm M1 and M2 frame with 2.2 \times 2.2 μm square opening, 0.6 μJ , spot size : 2.1 μm in 1/e² diameter.

The simulation results with various sizes of vertical metallic make-link structures compared with experimental results are displayed in Fig. 8. It shows the relative process

window for each structure to compare with the experimental results. The graph demonstrates clearly that simulation results are consistent with the trend of the decreasing relative laser energy window with a decrease of link structure size. For structures with $0.5\mu\text{m}$, $1.2\mu\text{m}$, $2\mu\text{m}$ and $4\mu\text{m}$ lower metal line width, the relative process window were 0.7, 0.77, 0.91 and 0.96, respectively.

Simulation results show that a value of approximately 0.69 was extrapolated for relative energy process window of a zero width metal 1 line. This is a rather conservative result compared with the experimental result. The difference may be attributed to other practical factors such as lens effect, which will be discussed in more detail in the following section. As a result of both experiments and simulations, there appears to exist an acceptable energy process window for any scaled links as long as the lower metal line can share the metal with the resulting link sheet with sufficient electromigration reliability.

Another key factor is the smallest spot size and the alignment accuracy that the laser system can make. Simulations suggested that the spot size used in each linking process played an important role in deciding the process window. It was found to be important to decide the absorbed energy by metal 2 as well as that by metal 1 to have a broad process window. Efforts have been made to find the optimum ratio of the absorbed energy densities within metal 2 to metal 1, and the ratio was found to be around 40% to 50% in 2-D models, as determined by simulations.

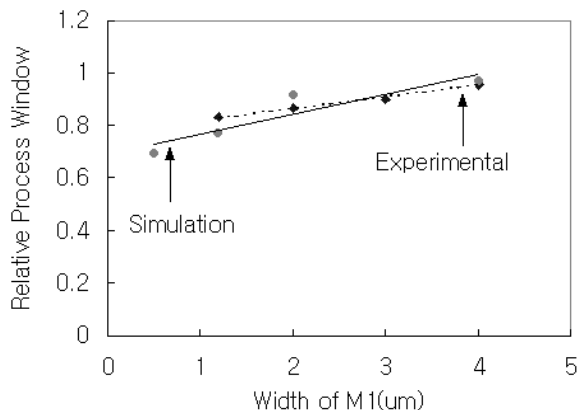


Fig. 8. Simulation results of make-linking showing relative process windows and calculated available energy ranges for different link structures.

We have learned that the laser energy absorbed in the upper metal frame enhances cracking from the upper corners of metal 1 and leads them to the inside lower corners of metal 2. However, too much energy absorbed in the upper metal frame will induce earlier passivation cracking, thereby decreasing the high end of process window. From simulations, it was observed that too small energy density absorbed in metal 2 frame, compared with the energy density absorbed in metal 1, caused another failure mode by cracking at a different point in the passivation, the center of metal 2 opening, instead of the cracking to the out-

TABLE II
LASER SPOT SIZE USED FOR SIMULATIONS (UNIT : μm)

W_{M1}	Gap	Spt $1/e^2$	Abs in M1	Abs in M2	Density Ratio in 2-D Model
4	1	7.2	0.46	0.23	0.5
2	1	4.8	0.30	0.24	0.5
1.2	0.5	3.1	0.26	0.36	0.4
0.5	0.5	2.1	0.11	0.35	0.4

- W_{M1} : Width of metal 1 line.
- Spt : Spot size in $1/e^2$ diameter.
- Abs : Ratio of energy absorption in each metal line to total effective laser energy.
- Density Ratio : Relative laser energy density ratio on the top surface of metal 2 frame to that of metal 1 line in 2-D model.

side of the upper metal frame. This can be considered as the passivation damage caused by the lower metal cracking mixed up with upper corner cracking from metal frame in the direction of the metal 2 opening. This failure was not experimentally observed because all structures were irradiated by laser pulses with the spot size equal to about twice the width of each lower metal line in order to have a uniform temperature distribution throughout the top surface of metal 1. Therefore, this does not lower the ratio of energy density absorbed in metal 2 which might otherwise cause the different failure mode.

In the case of large links (structures with 2, or $4\mu\text{m}$ wide metal 1 line), a ratio of around 50% in 2-D model was found to give a broad process window. For scaled links ($0.5\mu\text{m}$, or $1.2\mu\text{m}$ wide metal 1), a ratio of 40% or so was sufficient for the ratio of energy density in metal 2 to metal 1. This is because more energy is needed to initiate the cracking from metal 1 with a smaller line width. Assuming Gaussian distribution in TEM_{00} mode, the irradiance at a distance from center, r , is described by

$$I_r = I_0 \times \exp(-2r^2/w^2) \quad (1)$$

- w : Spot size in $1/e^2$ diameter.

Based on this equation, the optimum spot size can be decided from the ratio of energy density on the surface of metal 2 to that of metal 1 in 2-D model. Table II shows the spot sizes used for simulations of various links to get broad process windows. It is noted that energy density values in the table were calculated based on the 2-dimensional finite element models and the width of metal 2 frame was fixed as $2\mu\text{m}$ throughout the simulation. The absorption in each metal is shown relative to the total effective energy. Lens effect was ignored in these calculations and the substrate damage from the gap was assumed to be negligible.

The spot size was selected to find the specific ratio of energy densities of metal 2 to metal 1 in the finite elements model, around 40% to 50%, and this was the criterion in

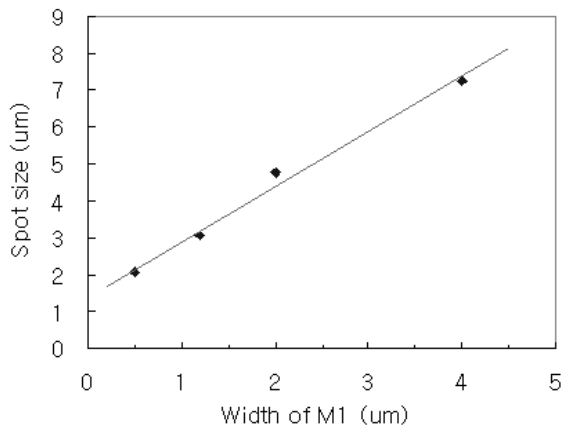


Fig. 9. Optimum spot size calculation, spot size in $1/e^2$ diameter.

the decision of spot size. From table II, the energy density irradiated in metal 2 does not vary that much compared with that in metal 1. This means there exists a narrow range of optimum energy density for metal 2 frame. However, higher energy density is needed for linking of a scaled make-link because of the small metal 1 line as mentioned earlier.

Fig. 9 displays the optimum spot size in $1/e^2$ diameter for various make-link structures from the results of simulations. The following is a simple equation to evaluate the optimum spot size in $1/e^2$ diameter acquired from the curve in Fig. 9.

$$S_{opt} = 1.49 \times W_{M1} + 1.48 \quad (2)$$

- S_{opt} : Spot size in $1/e^2$ diameter.
- W_{M1} : Width of metal 1 line.

Equation 2 demonstrates the importance of a laser systems ability to decrease the spot size with acceptable alignment accuracy for the processing of scaled links. However, considering the lens effect due to the step of unplanarized passivation, the acceptable spot size is considered to be slightly larger than the calculated value for each structure.

Modern IR laser systems are being designed to focus a round $1/e^2$ spot size as small as $1.7 \mu\text{m}$ or less in diameter with an alignment accuracy of $0.3 \mu\text{m}$ and the spot size tends to decrease even more. Therefore, these spot size and alignment accuracy would enable the scaled link with $0.5 \mu\text{m}$ wide metal 1 line and a metal 2 frame with $1.5 \times 1.5 \mu\text{m}$ square opening to be possible for linking with an acceptable process window. Furthermore, green laser systems can be focused to a $1 \mu\text{m}$ spot size or so in $1/e^2$ diameter, thereby, allowing further scaling potential of make link structure.

A. Metal Frame Gap

As a design factor, the metal 1 - metal 2 gap (M1-M2 gap) was also investigated to see the effect on the laser process. The structures with a $4 \mu\text{m}$ wide line and $4 \times 4 \mu\text{m}$ opening (zero gap) were irradiated by laser pulses with

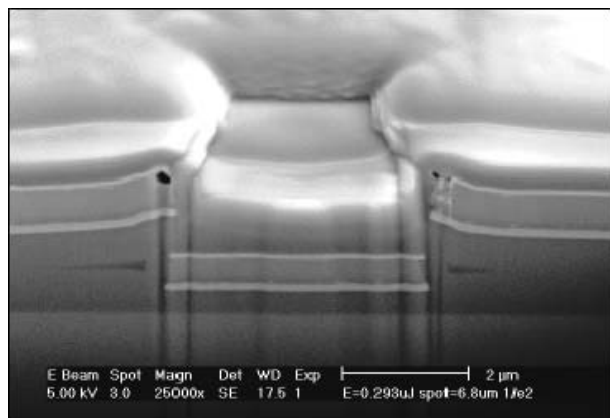


Fig. 10. Voids found at the upper frame corners for a vertical link with $4 \mu\text{m}$ metal 2 opening, $4 \mu\text{m}$ metal 1 line (zero gap), exposed to a laser pulse of a $0.293 \mu\text{J}$ energy and a $6.8 \mu\text{m}$ spot in $1/e^2$ diameter.

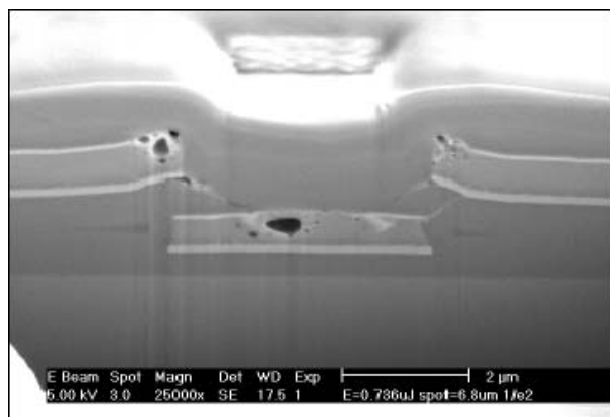


Fig. 11. For the zero gap structure ($4 \times 4 \mu\text{m}$ metal 2 opening and $4 \mu\text{m}$ metal 1 line), two link sheets were formed at $0.736 \mu\text{J}$ with a $6.8 \mu\text{m}$ spot in $1/e^2$ diameter. One link was first formed downward from the lower corners of the metal 2 frame, then the second one was formed upward from the upper corners of the metal 1 line.

various energies and a $6.8 \mu\text{m}$ spot size in $1/e^2$ diameter. Results show that no link is formed until $0.40 \mu\text{J}$, even though voids have been found at the corners of the upper frame at a much lower laser energy of $0.293 \mu\text{J}$, as shown in Fig. 10. When the laser energy is increased to $0.55 \mu\text{J}$, cracking was observed to occur from the lower corners of the frame where the link is formed downward to the metal 1 line.

At an energy of $0.736 \mu\text{J}$, the downward links from metal 2 touched the center of metal 1 line. In the mean time, the lower metal started to melt and the second link sheet was formed upward from the upper corners of metal 1, as shown in Fig. 11. The link formed in such a way is not stable and the energy absorbed by the frame can easily crack the passivation, therefore, the overall reliability of this type of link should not be high enough.

In order to compare the link formation process of link structures with the same metal 1 line width and metal 2 frame width but with a $1 \mu\text{m}$ M1-M2 gap (Sample 3) were processed with the same energy range and a spot size of

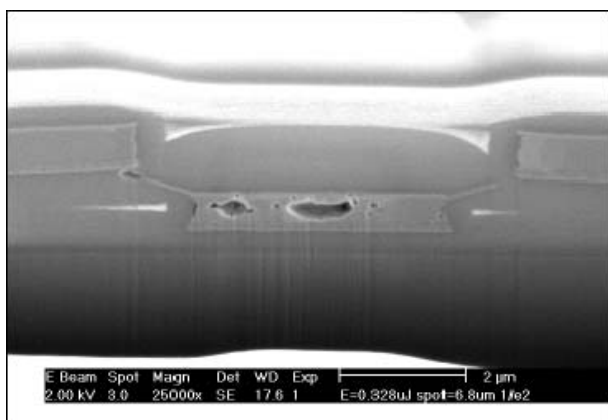


Fig. 12. Vertical link structure with a 4 μm metal 1 line and 6 μm metal 2 opening. Links were successfully formed at 0.328 μJ with a 4 μm $1/e^2$ spot. This link structure shows extremely high yield at an optimal energy around 0.7 μJ .

6.8 μm in $1/e^2$ diameter. FIB cross sections indicated that solid links were successfully formed at 0.328 μJ as can be seen in Fig. 12. No passivation crack was found until the laser energy reached 1.0 μJ . The range of energy process window where acceptable links form is determined to be from 0.33 to 1.0 μJ and this is much broader than for the case of zero-gap structure with the same metal 1 line width and metal 2 frame width.

Considering the Gaussian distribution of a laser pulse impinging on a link structure with a 4 μm metal 1 line, a 4 \times 4 μm metal 2 opening (gap=0 μm) and a frame width of 2 μm , 38.4 % of the total energy absorption is calculated to be absorbed by the metal 2 frame, if the $1/e^2$ laser spot size is set equal to about twice the line width of metal. Thus, the high end of the energy process window should be lowered significantly due to the increased probability of frame damage. On the other hand, for the structure with a 1.0 μm gap between metal 1 and metal 2, the frame-absorbed energy decreases to 14.2 % and around 15 % of the total laser energy absorption is transmitted through the gap. As a result, the frame can tolerate more energy before being damaged.

Furthermore, the TEOS re-flow process during fabrication, which was the old standard planarization process, was not able to fully planarize the steps caused by the multilevel metallization processes. The glass steps around the frame opening acts as an optical lens so that a part of the laser energy irradiating on the passivation steps can be refracted and absorbed by the side walls of the frame opening leaving a cool corner on the metal 1 line. It is very possible that the frame temperature near the opening is equal or even higher than the cool metal 1 corner. Hence, links could be initiated first from the lower corners of the upper metal frame.

For the structure with an M1-M2 gap, although the lens effect still exists, the energy absorbed by the metal 2 frame is much less than the energy absorbed by the metal 2 frame of zero-gap structures, which in turn elevates the critical laser energy for passivation damage. The 15 % leakage

of laser energy through the 1.0 μm wide gap would not become a concern for substrate damage because the total energy absorbed by the silicon substrate is relatively low for a multilevel metallization process.

V. CONCLUSIONS

It has been shown through experimental and simulation results that laser energy is the most critical factor controlling the link process. Moderate energy should be used to counterbalance the link formation and metal voiding. Laser energy process windows for different structures were extracted considering both measured resistance and microscopic analysis and also simulated using finite elements models. The results suggest that the laser-induced vertical metallic link is seamless for the application to current VLSI technology in the aspect of relative energy process window of scaled links. It is shown that a M1 - M2 gap is required to reduce the energy absorption on the frame and decrease the lens effect on M1 which lowers the temperature of the corners of M1. Finally, an acceptable process window will be expected for deeply scaled link structures with an improvement of quality of laser processing technology.

REFERENCES

- [1] J. B. Bernstein, W. Zhang, and C. Nicholas, "Laser formed metallic connections," *IEEE Trans. Comp. Packag. Manufact. Technol. Part B*, vol. 21, no. 2, pp. 194-196, 1998.
- [2] J. B. Bernstein, W. Zhang, and C. Nicholas, "Laser programmable vias," *IEEE Proc. International Interconnect Technology Conference*, p. 205, June, 1998.
- [3] W. Zhang, J. Lee, Y. Chen, J. B. Bernstein, and J. S. Suehle, "Reliability of laser-induced metallic vertical links," *IEEE Trans. Comp. Packag. Manufact. Technol.*, vol. 22, no. 4, pp. 614-619, 1999.
- [4] J. Lee, W. Zhang, and J. B. Bernstein, "Scalability study of laser-induced vertical make-link structure," *IEEE Trans. Semiconduct. Manufact.*, vol. 13, no. 4, pp. 442-447, 2000.
- [5] W. Zhang, X. Xie, and J. B. Bernstein, "Laser-formed vertical metallic link and potential implementation in digital logic integration," *Proc. Military and Aerospace Applications of Programmable Devices and Technologies Conference*, 1999, Unpublished.
- [6] I. A. Blech, "J. Appl. Phys.", vol. 47, pp. 1203, 1976.
- [7] T. Kikkawa, "Quarter-micron interconnection technologies for 256m drams," *Extended Abstracts of the 1992 International Conference on Solid Devices and Materials*, pp. 90-92, 1992.
- [8] Y. Shen, S. Suresh, and J. B. Bernstein, "Laser linking of metal interconnects: Analysis and design considerations," *IEEE Trans. Electron Devices*, vol. 42, no. 3, pp. 402-410, 1996.